Systems & Control Transactions

Original Research Article
Peer Reviewed Conference Proceeding
ESCAPE 36 - European Symposium on Computer Aided Process Engineering
Sheffield, UK. 21-24 June 2026

PSE PRESS

Simulation of Fixed-Bed Reactor System for Combined Ca–Cu Chemical Looping with Integrated Combustion and CO_2 Capture

Levente Biró, Norbert-Botond Mihály, Ana-Maria Cormoș*

Babeș – Bolyai University, Department of Chemical Engineering, Cluj-Napoca, Romania
* Corresponding Author: ana.cormos@ubbcluj.ro

ABSTRACT

As greenhouse gas emissions accelerate global warming, new capture and storage technologies are essential for reducing the industrial CO_2 concentration in the atmosphere. This study addresses the urgent need for greenhouse gas capture technologies by developing a detailed dynamic mathematical model for Chemical Looping Process with Integrated Combustion and CO_2 capture (CL-ICCC). In the CL-ICCC process configuration, CO_2 capture is integrated into the chemical looping combustion system, resulting in a higher-purity, more efficient process. In this work Cu/CuO oxygen carrier material and $CaO/CaCO_3$ sorbent materials were considered in a fixed bed reactor as solid phase to investigate Oxidation and Reduction/Calcination processes under different operating conditions. The simulation results were compared with experimental results from the literature. In case of the oxidation process, a sensitivity study was performed to investigate the behavior of the process for variation of different operating parameters under dynamic conditions: gas composition, initial gas temperature and solid phase mass composition. In the case of reduction/calcination, multiple fuel type and solid composition were investigated.

Keywords: Carbon Dioxide Capture, Chemical Looping, Fixed-Bed Reactor, Hydrogen generation, Sensitivity Study

INTRODUCTION

In the last years, the level of greenhouse gases (GHG) increased drastically, accelerating the process of global warming by raising the average temperature. [1] To create a pollution-free world, it is impossible to minimize all major pollution sources, such as industrial, transportation or agricultural GHG emissions. New GHG capture technologies, specifically CO_2 capture methods, that can have a negative, reducing effect on overall greenhouse gas levels are the solution. [2] Chemical Looping Combustion (CLC) is one of these new types of solutions and it can be adapted in multiple ways. The main purpose is to reduce GHG level in flue gas after the industrial processes. The working principle of the process is very simple: the process uses two different reactors: an Air Reactor (AR) where an oxidation process takes place between a metal or metal-oxide (known as Oxygen Carrier (OC)) and a Fuel Reactor (FR) where the combustion process can be performed in the absence of air. [3-5] An upgraded version of CLC process is the Chemical Looping with Integrated Combustion and CO_2 Capture (CL-ICCC) process. In this case the CO_2, which will be captured, is generated during the main process and that can increase the efficiency of the plant, also minimizing the climate change effect. [6] However, the products of the CL-ICCC process can be stored and used as raw materials for different processes, depending on the market and the plant operating profile. The main products of the CL-ICCC plant are pure H_2, CO_2 gas and electric power via steam. [7-9] The flowsheet of the presented, complex chemical process can be seen in Figure 1. All chemical processes take place in a single fixed-bed reactor. A complex valve system, illustrated in Figure 1, is included to switch between the different gaseous raw materials. In this study a copper-based OC, more specifically Cu/CuO material is used. For the CO_2 capture process the Ca-based compound is an optimal and efficient choice from an economic point of view. [9] The main objective

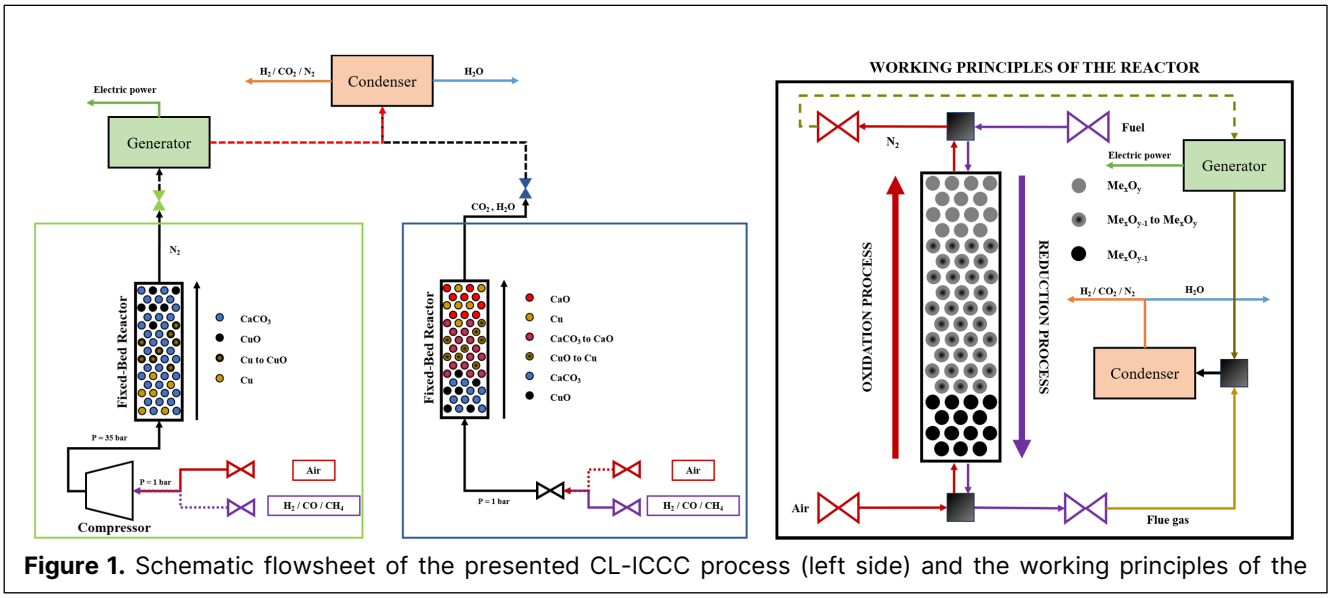

Figure 1. Schematic flowsheet of the presented CL-ICCC process (left side) and the working principles of the

of this work is to develop a dynamic mathematical model of the entire CL-ICCC process which can be divided into three different parts.

Carbonation process (A)

The H_2 synthesis occurs based on the reaction equations (1) – (3). At the same time the in-situ CO_2 capture takes place. As output of the system, the gaseous phase contains a significant quantity of H_2 gas, high-pressure steam, with fuel traces. The chemical process is performed in Fixed-Bed Reactors via Steam Enhanced Reforming (SER) and Water Gas Shift (WGS) processes [9, 10].

$$CH_4 + H_2O \rightarrow CO + 3\,H_2 \quad (1)$$

$$CO + H_2O \rightarrow CO_2 + H_2 \quad (2)$$

$$CH_4 + 2\,H_2O \rightarrow CO_2 + 4\,H_2 \quad (3)$$

$$CaO + CO_2 \rightarrow CaCO_3 \quad (4)$$

Oxidation (Regeneration) process (B)

The regeneration of the OC material (according to the equation 5) takes place in the oxidation process. The OC capability and type have a high influence on the efficiency of the carbonation process [11, 12]. During the chemical process, the oxidation stage generates a high amount of energy, and the excess energy can be used in steam generation, according to the scientific work of J. R. Fernández et al. [9].

$$2\,Cu + O_2 \rightarrow 2\,CuO \quad (5)$$

Calcination (reduction) process (C)

During the calcination process, the CO_2 gas is generated via two different ways: from the decomposition of the calcium carbonate, which was generated during the carbonation process and from the reaction between syngas and OC material [7, 11, 13]. The reactions described in equations:

$$4\,CuO + CH_4 \rightarrow 4\,Cu + CO_2 + 2\,H_2O \quad (6)$$

$$CuO + H_2 \rightarrow Cu + H_2O \quad (7)$$

$$CuO + CO \rightarrow Cu + CO_2 \quad (8)$$

$$CaCO_3 \rightarrow CaO + CO_2 \quad (9)$$

After the calcination process, the reactor remains at elevated temperature, due to the excess heat generated during the reduction stage and not consumed in the calcination. To improve overall efficiency, syngas synthesis can be performed immediately after the reduction, supplying fuel for subsequent or parallel reduction cycles.

MATERIALS AND METHODOLOGY OF THE RESEARCH

The aim of this study was to develop a dynamic mathematical model describing stages B and C, with emphasis on model validation and sensitivity analysis of key operating parameters. Although CO_2 capture and storage processes are well documented in the literature, differences arise in the choice of oxygen carrier and CO_2 sorbent, as well as in the level of model detail. J. R. Fernández et al. proposed several models for the same industrial process; however, their pseudo-homogeneous formulations simplify the temperature profile and provide only limited description of gas–solid interactions. [7-10, 12]

In stage B, a critical parameter is the stability of the solid phase under high-temperature and high-pressure conditions. Reactor temperatures may exceed 1000 °C and pressures approach 35 bar, emphasizing the need for appropriately selected support materials. To simulate the chemical process, the initial step involved validating

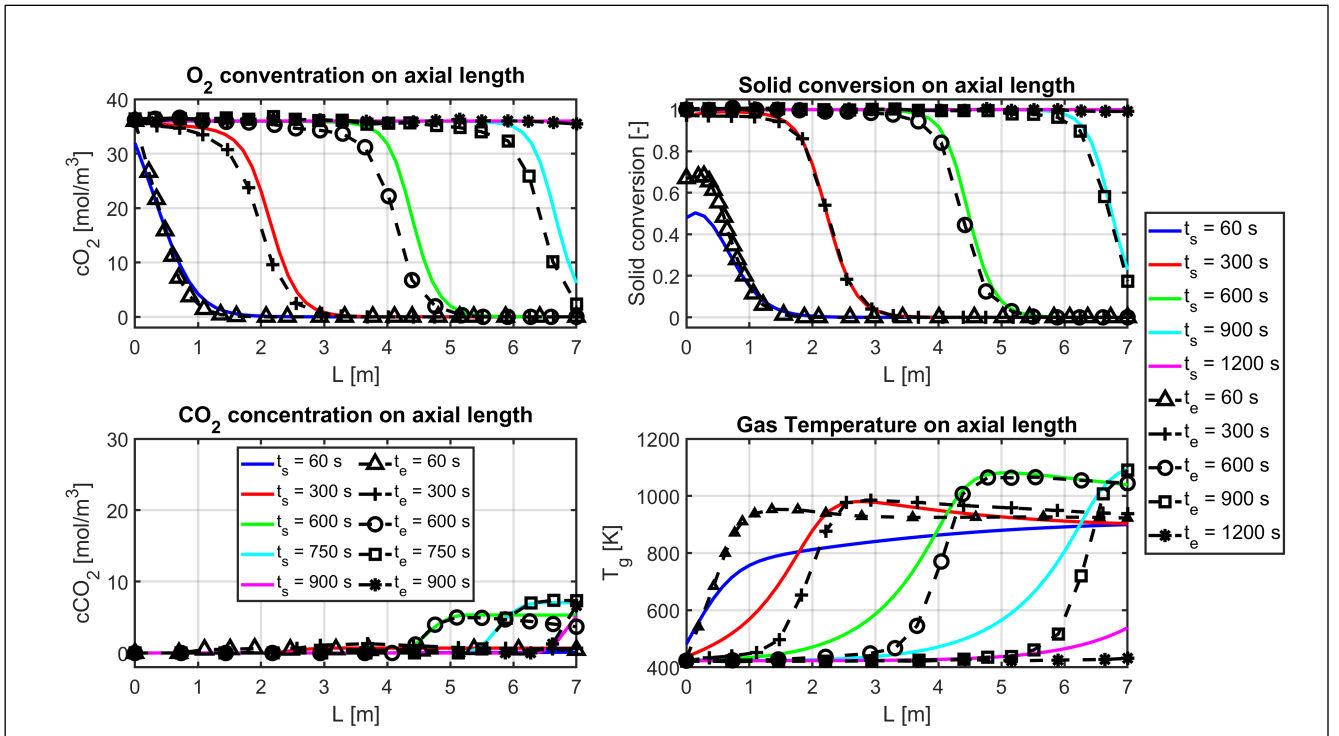

Figure 2. Validation diagrams of the stage B process (solid composition: Cu:Ca = 0.28:0.23) (simulated results vs.

the reaction kinetics under various conditions using experimental data from the literature. F. García-Labiano et al. conducted a comprehensive kinetic study on copper-based oxygen carriers, through first-order kinetic model, was chose for this work. [14]

Table 1. Kinetical parameters of Stage B and Stage C. [14, 15]

Parameters	U.M.	Values
Stage B		
$\rho_{m,Cu}$	kmol/m^3	140.252
L_{Cu}	m	$4 \cdot 10^{-10}$
$k_{0,ox}$	m/s	$4.7 \cdot 10^{-6}$
$E_{a,ox}$	kJ/mol	15
Stage C		
$\rho_{m,CuO}$	kmol/m^3	80.402
L_{CuO}	m	$2.3 \cdot 10^{-10}$
k_{0,H_2}	m/s	$1 \cdot 10^{-4}$
E_{a,H_2}	kJ/mol	33
$k_{0,CO}$	m/s	$5.9 \cdot 10^{-6}$
$E_{a,CO}$	kJ/mol	14
k_{0,CH_4}	m/s	$4.5 \cdot 10^{-4}$
E_{a,CH_4}	kJ/mol	60
$k_{0,red}$	kmol/(m^3 • s)	252 015
$E_{a,red}$	kJ/mol	91.7

Although the previous studies provided a solid theoretical foundation, several literature sources indicate that the oxidation process is more accurately represented by a second-order kinetic model. In this formulation, key parameters include the oxygen-carrier layer thickness (L_{Cu}) and its density ($\rho_{m,Cu}$), as shown in equation (10) and (11):

$$\upsilon_{p_{ox}} = \frac{dX}{dt} = \frac{2}{\tau} \cdot (1 - X_{ox})^{0.5} \quad (10)$$

$$\tau = \frac{L_{Cu} \cdot \rho_{m,Cu}}{b \cdot k_{ox} \cdot C_g^n} \quad (11)$$

$$k_{ox} = k_{0,ox} \cdot e^{\left(-\frac{E_{a,ox}}{RT}\right)} \quad (12)$$

where X_{ox} is the conversion of the solid component, b is the stoichiometric factor of reaction, k_{ox} is the chemical reaction rate constant of the oxidation process [m/s], C_g is the gas component concentration in the reactor chamber [kmol/m^3], n is the reaction order, τ is the necessary time to complete the solid conversion [s], R is the gas constant [J/mol•K]. The reaction rate constant is calculated by the Arrhenius equation (12).

For calcination, additional parameters have been defined in the literature to account for temperature effects, maximum conversion, and the equilibrium CO_2 concentration in the system, as expressed in equation (13) and (14):

$$\upsilon_{p_{cal}} = \frac{dX_{cal}}{dt} = k_{cal} \cdot (1 - X_{cal})^{\frac{2}{3}} \cdot \left(c_{CO_2,eq} - c_{CO_2}\right) \quad (13)$$

$$c_{CO_2,eq} = \frac{5.045 \cdot 10^8}{T} \cdot \exp\left(-\frac{20474}{T}\right) \quad (14)$$

$$k_{cal} = k_{0,cal} \cdot e^{\left(-\frac{E_{a,cal}}{RT}\right)} \quad (15)$$

where X_{cal} is the conversion of the solid component in the calcination process, k_{cal} is the chemical reaction rate constant [kmol/(m³•s)], c_{CO_2} is the CO_2 concentration in the reactor chamber [kmol/m³], $c_{CO_2,eq}$ is the equilibrium concentration of the CO_2 gas, calculated by equation (14), according to J. M. Alarcón et al. [13] The reaction rate constant is evaluated using the Arrhenius equation (15). The full set of kinetic parameters used in this work is summarized in Table 1.

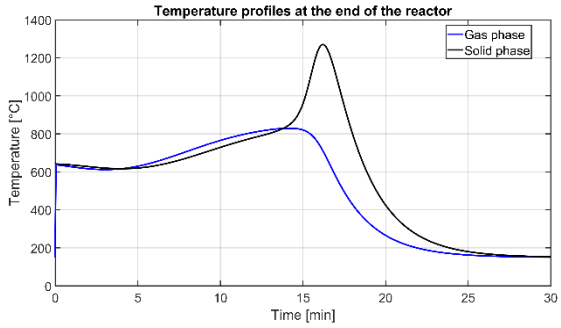

Figure 3. Temperature profiles at reactor exit are in a steady state regime.

For the model development, the governing equations were formulated using standard mass and energy balance relationships, consistent with established literature. In stage B, J. R. Fernandez et al. proposed two alternative modelling approaches, noting that the elevated temperatures reached during oxidation may induce partial calcination. [12] To examine this effect, they developed two different models: one model when the calcination reaction is not considered during the process and an other model when it is considered. In this study, the mathematical model was performed based on the second case. The components mass balance equations are presented via equations (16) – (22):

$$\varepsilon\frac{dm_{Cu}}{dt} = -(1-\varepsilon)\bullet\eta\bullet v_{p_{ox}}\bullet m_{Cu} \quad (16)$$

$$\varepsilon\frac{dm_{CuO}}{dt} = (1-\varepsilon)\bullet\eta\bullet v_{p_{ox}}\bullet m_{Cu}\bullet\frac{M_{CuO}}{M_{Cu}} \quad (17)$$

$$\varepsilon\frac{dm_{CaCO_3}}{dt} = -(1-\varepsilon)\bullet v_{p_{cal}}\bullet m_{CaCO_3} \quad (18)$$

$$\varepsilon\frac{dm_{CaO}}{dt} = -(1-\varepsilon)\bullet v_{p_{cal}}\bullet m_{CaO}\bullet\frac{M_{CaO}}{M_{CaCO_3}} \quad (19)$$

$$\varepsilon\frac{dc_{O_2}}{dt} = -w_g\bullet\frac{dc_{O_2}}{dz} - \frac{(1-\varepsilon)\bullet\eta\bullet v_{p_{ox}}\bullet m_{Cu}}{2\bullet M_{Cu}\bullet A\bullet dz} \quad (20)$$

$$\varepsilon\frac{dc_{N_2}}{dt} = -w_g\bullet\frac{dc_{N_2}}{dz} \quad (21)$$

$$\varepsilon\frac{dc_{CO_2}}{dt} = -w_g\bullet\frac{dc_{CO_2}}{dz} + \frac{(1-\varepsilon)\bullet v_{p_{cal}}\bullet m_{CaO}}{M_{CaCO_3}\bullet A\bullet dz} \quad (22)$$

where m_j is the mass of the *j* component in the solid bed (*j* = Cu, CuO, CaO, $CaCO_3$) [kg], η is an efficiency factor of the chemical reaction, ε is the solid bed porosity, c_i is the concentration of the *i* components in the reactor (*i* = O_2, N_2, CO_2) [kmol/m³], M_j is the molecular weight of the *j* component [kg/kmol], w_g is the velocity of the gas flow [m/s], A is the cross section of the reactor [m²], dz is the length of a section of the reactor (the reactor length was divide into 50 equal spaces).

The energy balance equations describe the conventional heat exchange between the solid and gaseous phases, according to the plug flow reactor operating principles. The balance equations are presented below:

$$\varepsilon\frac{dT_g}{dt} = -w_g\bullet\frac{dT_g}{dz} - \frac{K_T\bullet A_T\bullet(T_g-T_s)}{c_{p_g}\bullet\rho_g\bullet A\bullet dz} \quad (23)$$

$$\varepsilon\frac{dT_s}{dt} = \frac{K_T\bullet A_T\bullet(T_g-T_s)}{c_{p_s}\bullet\rho_s\bullet A\bullet dz} - \sum\frac{(1-\varepsilon)\bullet\eta\bullet\Delta H_x\bullet v_{p_x}\bullet m_j}{b\bullet M_j\bullet c_{p_s}\bullet\rho_s\bullet A\bullet dz} \quad (24)$$

where T_s is the temperature of the solid bed [K], T_g is the temperature of the gaseous phase [K], K_T is the heat transfer coefficient [W/m²K], A_T is the surface area where the heat exchange process takes place [m²], c_{p_s} and c_{p_g} are the specific heat capacity for the gaseous and solid phases [J/kgK], ρ_s and ρ_g are the density of the gaseous and solid phases [kg/m³], x is an indicator for the processes during the interpretation of the energy balance equations (x = oxidation or calcination).

Table 2. Process operating parameters.

Parameters	Values
Stage B	
Initial gas temperature [$T_{g,0}$]	423 K
Initial solid temperature [$T_{s,0}$]	923 K
Pressure [P]	35 bar
Inlet mass flow velocity [Q_s]	21 kg/m²s
Process effectiveness [η]	0.3
Inlet O_2 concentration [$c_{O_{2_{in}}}$]	3.6 %
Particle size [d_p]	10 mm
Porosity [ε]	0.5
Solid phase density [ρ_s]	3400 kg/m³
Cu weight fraction [ρ_{Cu}]	950 kg/m³
$CaCO_3$ weight fraction [ρ_{CaCO_3}]	750 kg/m³
Stage C	
Initial gas temperature [$T_{g,0}$]	973 K
Initial solid temperature [$T_{s,0}$]	973 K
Pressure [P]	1 atm
Inlet molar flow velocity [Q_s]	1 kmol/s
Process effectiveness [η]	0.8
Inlet fuel gas concentration [$c_{i_{in}}$]	75 %
Particle size [d_p]	5 mm
Porosity [ε]	0.5
Solid phase density [ρ_s]	2330 kg/m³

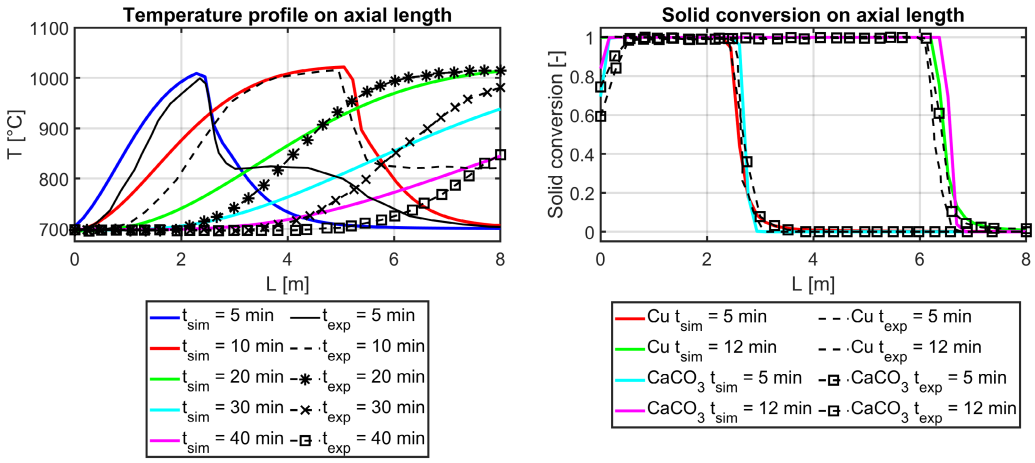

Figure 4. Validation diagrams of the stage C during H_2 process (solid composition: Cu:Ca = 0.3:0.15) (simulated results vs. experimental results)
From left to right: 1. Gas temperature profile on axial length; 2. Solid conversion on axial length;

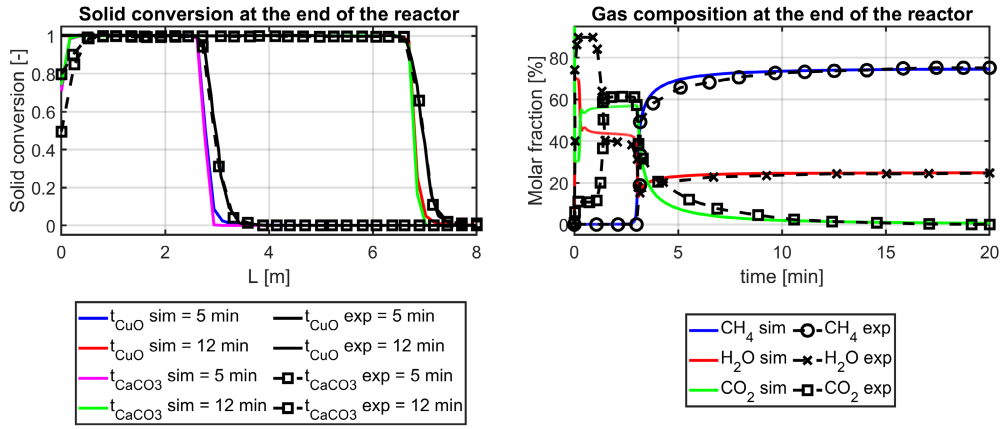

Figure 5. Validation diagrams of the stage C during CO and CH_4 process (solid composition: Cu:Ca = 0.3:0.21). (simulated results vs. experimental results)

For the calcination processes, the defined equations are the same, the differences come from the direction of the chemical reactions, from the raw material to the product, according to the reaction equations (6 - 9). The developed mathematical model is also operating in adiabatic conditions, where the energy for the calcination process is generated in situ via the reduction processes. The mass and energy balance equations are described below:

$$\varepsilon \frac{dm_j}{dt} = \pm (1-\varepsilon) \bullet \eta \bullet \upsilon_{p_{red}} \bullet m_j \quad (25)$$

$$\varepsilon \frac{dc_i}{dt} = -w_g \bullet \frac{dc_i}{dz} \pm \frac{(1-\varepsilon) \bullet \eta \bullet \upsilon_{p_{red}} \bullet m_j}{b \bullet M_j \bullet A \bullet dz} \quad (26)$$

$$\varepsilon \frac{dT_g}{dt} = -w_g \bullet \frac{dT_g}{dz} - \frac{K_T \bullet A_T \bullet (T_g - T_s)}{c_{p_g} \bullet \rho_g \bullet A \bullet dz} \quad (27)$$

$$\varepsilon \frac{dT_s}{dt} = \frac{K_T \bullet A_T \bullet (T_g - T_s)}{c_{p_s} \bullet \rho_s \bullet A \bullet dz} - \sum \frac{(1-\varepsilon) \bullet \eta \bullet \Delta H_x \bullet \upsilon_{px} \bullet m_j}{b \bullet M_j \bullet c_{p_s} \bullet \rho_s \bullet A \bullet dz} \quad (28)$$

where i = H_2, H_2O, CO, CO_2, CH_4.

The model simulation was performed in MATLAB/Simulink, the used solver was 'ode15s'. The operating parameters (Table 2) were chosen based on multiple literature sources. [8, 12, 13]

DYNAMIC SIMULATIONS' RESULTS AND DISCUSSION

Dynamic simulation and sensitivity study of stage B

The dynamic mathematic simulation was conducted to evaluate the systems' behavior under realistic operating conditions. The oxidation reaction concluded at approximately 15 minutes, after which the system began to cool due to heat transfer between the fresh gas stream and the oxidized solid phase. Owing to the elevated temperature, a minor extent of $CaCO_3$ decomposition occurred, by the calcination process. Since the minimum

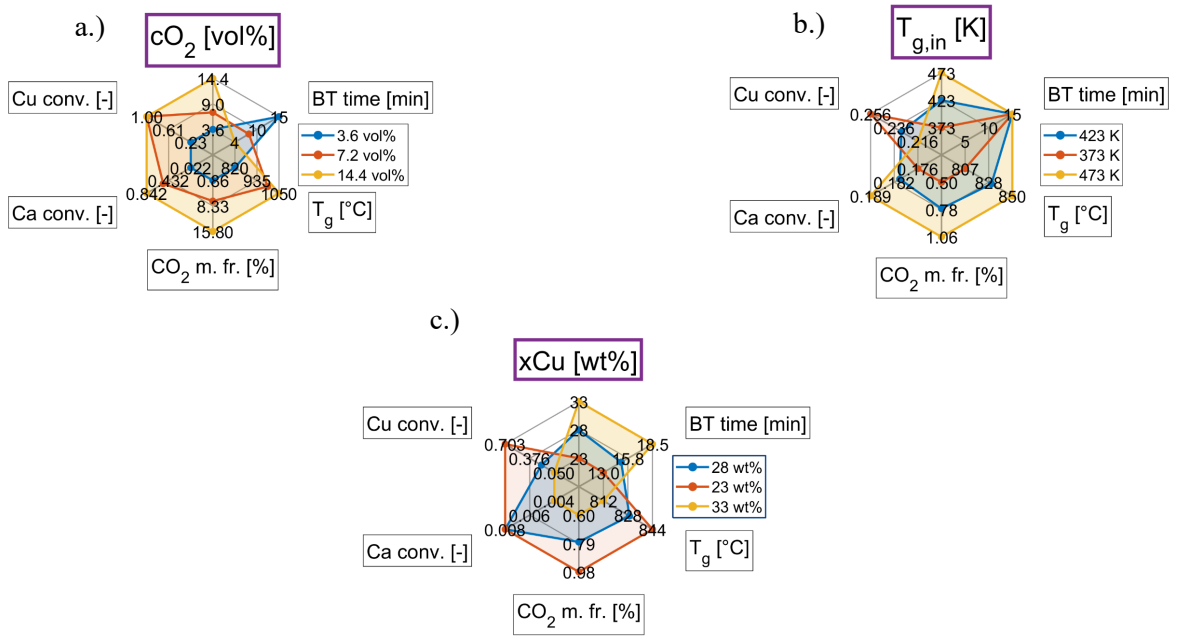

Figure 6. Spider web diagrams of the sensitivity study of the stage B (BT time is Breakthrough time): a.) Variation of gas composition [3.6 – 14.4 vol%]; b.) Variation of the initial gas temperature [373 – 473 K]; c.) Variation of the mass composition of the solid bed [23 – 33 wt% Cu];

temperature of the calcination exceeds 973 K, the peak temperature reached during stage B surpassed and threshold. The oxygen carrier achieved complete conversion at around 15 minutes, marking the breakthrough point. Beyond this point, the O_2 concentration returned to its initial level, signaling the end of the chemical reaction.

The steady state of the system within the reactor can be evaluated at two levels: the chemical composition and temperature. Figure 3 illustrates the temperature profiles of the solid and gas phases from the beginning to the breakthrough point. The temperature difference in the system is significant: the oxidation reaction generates a large amount of energy, and this energy is transferred to the gaseous phase to warm up the gas mixture to the operating temperature. After the breakthrough point, the temperature in the solid phase rises, caused by the excess heat from the oxidation process at the end of the undesired calcination process.

To investigate the system's response to variation in operating conditions, sensitivity analysis was performed. Three key parameters were examined: gas composition, initial gas temperature and mass difference in the case of Cu after 5 minutes on 2.5 m examination point. Based on the results, the hydrogen level can generate a non-favorable system behavior. The increase in O_2 concentration has a significant effect on system behavior, as illustrated in Figure 6. Higher hydrogen levels accelerate the reaction rate, resulting in shorter breakthrough times and an earlier appearance of the breakthrough curves. This intensified reaction also causes a significant temperature increase. At 14.4 vol% O_2, the peak gas-phase temperature is approximately 1, 050 °C, which is about 30% higher than under the reference operating conditions. At this point, the CO_2 concentration increases to 15.8 %, and the overall conversion of the Ca-based sorbent reaches 0.842 after 5 minutes at 2.5 m axial length. These conditions are undesirable, because the primary objective is to fully oxidize the oxygen carrier, while preserving the chemical integrity of the calcium-containing material. A lower initial gas temperature generates more desired results by higher Cu conversion and significantly lower Ca conversion. This phenomenon is caused by the temperature differences between the gas and the solid phase. The solid composition is also an important aspect of the system design and has significant impact on multiple evaluated parameters. A lower Cu composition in the solid bed causes a higher peak temperature, a shorter reaction time and a higher CO_2 level at the end of the reactor. The results indicate to estimate an optimized operating time, to decrease the appearance of the calcination in the oxidation process and maximize the Cu conversion.

Dynamic simulation of stage C

In the stage C, the chemical reaction is dictated by the composition of the fuel gas. Although the theoretical optimum operates with syngas ratio $CO:H_2$ = 1:3, trace alkanes (specifically CH_4) may be present due to valve malfunction or post-breakthrough operations. In order to develop a well-defined mathematical model, it is necessary to consider every case and perform three different

operating mods. Each operating mode was performed in isolated conditions, during the simulation steam was added to the pure fuel gas to create an inert atmosphere. The simulations were performed using the model equations (24-29), and the reactor was considered as an adiabatic system (perfectly isolated), which reduces the number of thermodynamic phenomena in the system.

The H_2 process was simulated for 80 minutes to evaluate the solid conversion, the gas composition and the temperature profiles. The breakthrough point occurred at 15 minutes when the solid phase reaches the maximum conversion level and the system reached its peak temperature. The process started with preheated gaseous phase at 973 K, which was also the temperature of the solid phase. After the fuel gas was introduced into the reactor chamber, an initial fluctuation of the gas composition occurred.

The CO process simulation duration was 30 minutes, and the breakthrough point was achieved in 12 minutes. During the process, significant amount of the CO_2 was detected, by the oxidation of the CO gas from syngas and from the calcination process for dissociation of the $CaCO_3$. In contrast with the H_2 solution, the reaction heat which comes from the CO oxidation process is much higher. The highest temperature obtained during the CO simulation was close to 1, 250°C, compared to 875°C obtained during the H_2 process.

With the CH_4 fuel gas, the simulation was performed under 20 minutes, and the end of the chemical reaction was nearly 3 minutes, which is almost 10 times shorter than the operating time of the H_2 simulation. The conversion of the $CaCO_3$ did not reach the maximum conversion level, which could be achieved by increasing the gas composition or the gas stream flow rate.

In the case of the H_2 model, the simulation results were validated for multiple mass composition by the experimental data provided by J. M. Alarcón et al. [13]

CONCLUSION

In this work, multiple mathematical models were developed successfully under dynamical operating conditions for the oxidation and calcination/reduction processes. The validation process was performed by experimental data presented in literature. During the validation process, the developed model accurately predicted the gas composition and the temperature profile at the end of the reactor, as well as the axial length and solid conversion. However, a sensitivity study was performed to examine the response of the oxidation process under dynamic operating conditions. Specifically, the elevated O_2 concentration (14.4 vol%) in the fuel gas stream indicates an undesirable calcination process. During the oxidation on an elevated peak temperature (1050°C) can produce the same unfavorable phenomenon: 0.189 Ca conversion after 5 minutes at 2.5 m axial length.

The calcination process is highly influenced by the composition and type of the fuel used. In the case of H_2 reduction, the peak temperature of the system was 875°C, while in the CO calcination, the value of the peak temperature was 1250°C. The CH_4 reduction process was performed under 3 minutes due to the large amount of energy generated via fuel gas. In practice, these three calcination types take place simultaniously in the reactor chamber in, complicates the modeling process.

ACKNOWLEDGEMENTS

This work was supported by a grant from Foundation „Sapientia Hungariae" (Hungary), through the „Collegium Talentum" Scholarship Program.

AUTHOR IDENTIFIERS

Author ORCIDs:
Biró L: 0009-0003-2971-3776
Mihály NB: 0000-0002-0126-2657
Cormoș AM: 0000-0003-0832-0722

REFERENCES

1. Beuttler C, Charles L, Wurzbacher J. The role of direct air capture in mitigation of anthropogenic greenhouse gas emissions. Front. Clim. 1: (2019). https://doi.org/10.3389/fclim.2019.00010
2. Europena Commision. https://eur-lex.europa.eu/legal-content/EN/TXT/HTML/?uri=CELEX:52018DC0773
3. Hossain MM, de Lasa HI. Chemical-looping combustion (CLC) for inherent 2 separations—a review. Chemical Engineering Science 63:4433-4451 (2008). https://doi.org/10.1016/j.ces.2008.05.028
4. Daneshmand-Jahromi S, Sedghkerdar MH, Mahinpey N. A review of chemical looping combustion technology: fundamentals, and development of natural, industrial waste, and synthetic oxygen carriers. Fuel 341:127626 (2023). https://doi.org/10.1016/j.fuel.2023.127626
5. Abuelgasim S, Wang W, Abdalazeez A. A brief review for chemical looping combustion as a promising CO2 capture technology: fundamentals and progress. Science of The Total Environment 764:142892 (2021). https://doi.org/10.1016/j.scitotenv.2020.142892
6. Liu G, Lisak G. Cu-based oxygen carriers for chemical looping processes: opportunities and challenges. Fuel 342:127828 (2023). https://doi.org/10.1016/j.fuel.2023.127828
7. Alarcón AM, Fernández JR, Abanades JC. Study of

a Cu-CuO chemical loop for the calcination of $CaCO_3$ in a fixed bed reactor. *Chem Eng J* 325:208-220 (2017) http://dx.doi.org/10.1016/j.cej.2017.05.070
8. Fernández JR, Abanades JC, Murillo R. Modeling of sorption enhanced steam methane reforming in an adiabatic fixed bed reactor. *Chem Eng Sci* 84:1-11 (2012) http://dx.doi.org/10.1016/j.ces.2012.07.039
9. Fernández JR, Abanades JC, Murillo R, Grasa G. Conceptual design of a hydrogen production process from natural gas with CO2 capture using a ca–cu chemical loop. International Journal of Greenhouse Gas Control 6:126-141 (2012). https://doi.org/10.1016/j.ijggc.2011.11.014
10. Fernández JR, Abanades JC, Grasa G. Modeling of sorption enhanced steam methane reforming – Part II: Simulation within a novel Ca/Cu chemical loop process for hydrogen production. *Chem Eng Sci* 84:12-20 (2012) http://dx.doi.org/10.1016/j.ces.2012.07.050
11. Noorman S, Gallucci F, van Sint Annaland M, Kuipers JAM. Experimental Investigation of chemical-looping combustion in packed beds: a parametric study. *Ind Eng Chem Res* 50:1968-1980 (2011) https://dx.doi.org/10.1021/ie1019112
12. Fernández JR, Abanades JC, Murillo R. Modeling of Cu oxidation in adiabatic fixed-bed reactor with N_2 recycling in a Ca/Cu chemical loop. *Chem Eng J* 232:442-452 (2013) http://dx.doi.org/10.1016/j.cej.2013.07.115
13. Alarcón JM, Fernández JR. $CaCO_3$ calcination by the simultaneous reduction of CuO in a Ca/Cu chemical looping process. *Chem Eng Sci* 137:254-267 (2015) http://dx.doi.org/10.1016/j.ces.2015.06.030
14. García-Labiano F, de Diego LF, Adánez J, Abad A, Gayán P. Reduction and oxidation kinetics of a copper-based oxygen carrier prepared by impregnation for chemical-looping combustion. Ind. Eng. Chem. Res. 43:8168-8177 (2004). https://doi.org/10.1021/ie0493311
15. Martínez I, Grasa G, Murillo R, Arias B, Abanades JC. Kinetics of calcination of partially carbonated particles in a ca-looping system for co₂ capture. Energy Fuels 26:1432-1440 (2012). https://doi.org/10.1021/ef201525k